

1 **Deforestation in Amazonia impacts riverine carbon dynamics**

2

3 F. Langerwisch^{1,2}, A. Walz³, A. Rammig^{1,4}, B. Tietjen^{5,2}, K. Thonicke^{1,2}, W. Cramer⁶

4 ¹ Earth System Analysis, Potsdam Institute for Climate Impact Research (PIK), P.O. Box 60
5 12 03, Telegraphenberg A62, D-14412 Potsdam, Germany

6 ² Berlin-Brandenburg Institute of Advanced Biodiversity Research (BBIB), 14195 Berlin,
7 Germany

8 ³ Institute of Earth and Environmental Science, University of Potsdam, Karl-Liebknecht-Str.
9 24-25, D-14476 Potsdam-Golm, Germany

10 ⁴TUM School of Life Sciences Weihenstephan, Land Surface-Atmosphere Interactions,
11 Technische Universität München, Hans-Carl-von-Carlowitz-Platz 2, 85354 Freising,
12 Germany

13 ⁵ Biodiversity and Ecological Modelling, Institute of Biology, Freie Universität Berlin,
14 Altensteinstr. 6, D-14195 Berlin, Germany

15 ⁶ Institut Méditerranéen de Biodiversité et d'Ecologie marine et continentale (IMBE), Aix
16 Marseille Université, CNRS, IRD, Avignon Université, Technopôle Arbois-Méditerranée,
17 Bât. Villemin - BP 80, F-13545 Aix-en-Provence cedex 04, France

18

19 *Correspondence to:* F. Langerwisch (langerwisch@pik-potsdam.de)

20

21

22 **Abstract**

23 Fluxes of organic and inorganic carbon within the Amazon basin are considerably controlled
24 by annual flooding, which triggers the export of terrigenous organic material to the river and
25 ultimately to the Atlantic Ocean. The amount of carbon imported to the river and the further
26 conversion, transport and export of it depend on temperature, atmospheric CO₂, terrestrial
27 productivity and carbon storage, as well as discharge. Both, terrestrial productivity and
28 discharge, are influenced by climate and land use change. The coupled LPJmL and RivCM
29 model system (Langerwisch et al., 2015) has been applied to assess the combined impacts of
30 climate and land use change on the Amazon riverine carbon dynamics. Vegetation dynamics
31 (in LPJmL) as well as export and conversion of terrigenous carbon to and within the river
32 (RivCM) are included. The model system has been applied for the years 1901 to 2099 under
33 two deforestation scenarios and with climate forcing of three SRES emission scenarios, each
34 for five climate models. We find that high deforestation (BAU scenario) will strongly
35 decrease (locally by up to 90%) riverine particulate and dissolved organic carbon amount until
36 the end of the current century. At the same time, increase in discharge leaves net carbon
37 transport during the first decades of the century roughly unchanged only if a sufficient area is
38 still forested. After 2050 the amount of transported carbon will decrease drastically. In
39 contrast to that, increased temperature and atmospheric CO₂ concentration determine the
40 amount of riverine inorganic carbon stored in the Amazon basin. Higher atmospheric CO₂
41 concentrations increase riverine inorganic carbon amount by up to 20% (SRES A2). The
42 changes in riverine carbon fluxes have direct effects on carbon export, either to the
43 atmosphere via outgassing, or to the Atlantic Ocean via discharge. The outgassed carbon will
44 increase slightly in the Amazon basin, but can be regionally reduced by up to 60% due to
45 deforestation. The discharge of organic carbon to the ocean will be reduced by about 40%
46 under the most severe deforestation and climate change scenario. These changes would have
47 local and regional consequences on the carbon balance and habitat characteristics in the
48 Amazon basin itself but also in the adjacent Atlantic Ocean.

49

50 **1 Introduction**

51 The Amazon basin, defined as the drainage area of the Amazon River, covers approximately
52 six million square kilometres, and more than 70% of it is still covered with intact rainforest
53 (Nobre, 2014). The amount of carbon in biomass in Amazonian rainforest is estimated to be
54 $93 \pm 23 \times 10^{15}$ g C (Malhi et al., 2006). This biomass is stored in a wide range of diverse
55 habitats, including tropical rainforest and savannahs, as well as numerous aquatic habitats,
56 like lakes and wetlands (Goulding et al., 2003; Eva et al., 2004; Keller et al., 2009; Junk,
57 1997). The large diversity in habitats, partly already founded in the geologic formation of
58 Amazonia, leads to a high diversity of animal and plant species (Hoorn et al., 2010), making
59 the Amazon rainforest one of Earth's greatest collections of biodiversity.

60 The Amazon River, which floods annually large parts of the forest, plays an important role in
61 supporting the diversity of Amazonian ecosystems. The flooding is most decisive for the
62 coupling of terrestrial and aquatic processes by transporting organic material from the
63 terrestrial ecosystems to the river (Hedges et al., 2000). The input of terrigenous organic
64 material (Melack and Forsberg, 2001; Waterloo et al., 2006), acts, for instance, as fertilizer
65 and food source (Anderson et al., 2011; Horn et al., 2011), and is a modifier of habitats and
66 interacting local carbon cycles (Hedges et al., 2000; Irmiler, 1982; Johnson et al., 2006;
67 McClain and Elsenbeer, 2001). Across the Amazon basin, the outgassing carbon from the
68 river to the atmosphere and export of it to the ocean are the two most important processes that
69 have to be included, when assessing the effects on riverine carbon dynamics under climate
70 and land use change. Approximately 470×10^{12} g C yr⁻¹ is exported to the atmosphere as CO₂
71 (Richey et al., 2002), in comparison with about 32.7×10^{12} g C yr⁻¹ of total organic carbon
72 (TOC) is exported to the Atlantic Ocean (Moreira-Turcq et al., 2003). It is estimated that the
73 large scale outgassing of carbon from the Amazon River plays an important role in assessing
74 the future carbon balance of the Amazon basin, integrating riverine as well as terrestrial
75 processes.

76 Deforestation continues to be the largest threat to Amazonia. The transformation of tropical
77 rainforest to cropland and pasture impacts ecosystem stability profoundly due to altered
78 climate regulation and species richness (Foley et al., 2007; Lawrence and Vandecar, 2014;
79 Malhi et al., 2008; Spracklen et al., 2012). Until the year 2012 approximately 20% of the
80 original forest of the Brazilian part of the Amazon basin has been deforested, corresponding
81 to an area of about 750,000 km² (Godar et al., 2014; INPE, 2013). This deforestation was
82 mainly driven by the land expansion for soybean and cattle production and the expansion of
83 the road network (Malhi et al., 2008; Soares-Filho et al., 2006). Governmental and
84 conservation efforts have helped to decrease recent deforestation rates (Nepstad et al., 2014)
85 but economic instability might reverse this trend (Aguiar et al., 2016; Fearnside, 2015).
86 Deforestation also alters the soil stability and increases erosion (Yang et al., 2003). Together
87 with climate change effects and forest burning, land cover change is predicted to release
88 carbon at rates of $0.5-1.0 \times 10^{15}$ g C yr⁻¹ from this area (Potter et al., 2009). Furthermore, the
89 effects of deforestation on terrestrial carbon storage and fluxes persist several decades after
90 logging because the forest needs about 25 years to recover approximately 70% of its original
91 biomass, and at least another 50 years for the remaining 30% after abandonment of agriculture
92 (Houghton et al., 2000; Poorter et al., 2016).

93 Deforestation immediately reduces the terrestrial organic carbon pools, which fuel riverine
94 respiration (Mayorga et al., 2005), while increasing the velocity and amount of runoff, as well
95 as the discharge (Foley et al., 2002; Costa et al., 2003). Additionally, climate change alters
96 precipitation which then affects inundation patterns (Langerwisch et al., 2013), such as
97 temporal shifts in high and low water months and changes of inundated area. The combined
98 effects of deforestation and climate change have the potential to tremendously alter the
99 exported terrigenous carbon fluxes, the amount of carbon emitted to the atmosphere and
100 exported the ocean. The local export of terrestrial organic carbon to the river changes the
101 nutrient supply and therefore alters the habitat for riverine plants and animals, (Hamilton,
102 2010).

103 The aim of our study is to elaborate on these combined effects of climate change and
104 deforestation on the riverine carbon fluxes, on the export of organic material into the Atlantic
105 Ocean and on the outgassing of riverine carbon to the atmosphere. By considering the
106 interactions between riverine and terrestrial carbon processes a complete view on future
107 changes in the regional and basin-wide carbon balance can be achieved for the Amazon basin.
108 When referring to deforestation in this study, we mean the effects of replacing tropical forest
109 with soy bean fields and pasture, as well as the effects of newly established land use on
110 carbon cycling.

111 To address these issues basin-wide data are needed, which not only describe the current
112 situation but also assess future changes, expanding our knowledge obtained from on-site
113 measurements. To partly overcome these limitations we make use of the well-established
114 dynamic global vegetation model LPJmL together with the riverine carbon model RivCM.
115 While LPJmL (Bondeau et al., 2007; Gerten et al., 2004; Rost et al., 2008; Sitch et al., 2003)
116 provides plausible estimates for the carbon and water pools and fluxes within the coupled
117 soil-vegetation system, RivCM (Langerwisch et al., 2015) focuses on the export, conversion
118 and transport of terrestrial fixed carbon in the river and to the atmosphere and ocean. In
119 Langerwisch et al. (2015) the solely effects of climate change have been estimated. The
120 results of the mentioned study show that climate change causes a doubling of riverine organic
121 carbon in the Southern and Western basin while reducing it by 20% in the eastern and
122 northern parts towards the end of this century. In contrast, the amount of riverine inorganic
123 carbon shows a 2- to 3-fold increase in the entire basin, independent of the climate change
124 scenario (SRES). The export of carbon to the atmosphere increases on average by about 30%.
125 The amount of organic carbon exported to the Atlantic Ocean depends on the SRES scenario
126 and is projected to either decrease by about 8.9% (SRES A1B) or increase by about 9.1%
127 (SRES A2). The current study, which is an extension of Langerwisch et al. (2015) goes one
128 step further and investigates the combined effects of climate change and deforestation on the
129 riverine carbon dynamics. The coupled model LPJmL-RivCM was forced by several climate
130 change and deforestation scenarios that cover a wide range of uncertainties. We estimated
131 temporal and spatial changes in three riverine carbon pools as well as changes in carbon
132 emissions to the atmosphere and carbon export the ocean.

133 **2 Methods**

134 To assess the impacts of climate change and deforestation on riverine carbon pools and fluxes
135 in the Amazonian watershed we applied the model system of LPJmL and RivCM. RivCM is a
136 grid-based model that assesses the transport and export of carbon at monthly time steps and is
137 driven climate data and terrestrial carbon pools (Langerwisch et al., 2015). Climate inputs are
138 taken from different global climate model simulations driven by three SRES scenarios (A1B,
139 A2 and B1; Nakićenović et al., 2000). Terrestrial carbon inputs are calculated by the process-
140 based dynamic global vegetation and hydrology model LPJmL (Bondeau et al., 2007; Gerten
141 et al., 2004; Rost et al., 2008; Sitch et al., 2003). To estimate soil and vegetation carbon,
142 LPJmL uses the above mentioned climate data and a set of deforestation scenarios from a
143 regional projections by SimAmazonia (Soares-Filho et al., 2006). An overview of the
144 interconnection between the two models and the scenarios is given in

145 **Figure 1.**

146 **2.1 Model descriptions**

147 **2.1.1 LPJmL – a dynamic global vegetation and hydrology model**

148 The process-based global vegetation and hydrology model LPJmL (Bondeau et al., 2007;
149 Gerten et al., 2004; Rost et al., 2008; Sitch et al., 2003) simulates the dynamics of potential
150 natural vegetation and thus carbon pools for vegetation, litter and soil and corresponding
151 water fluxes, in daily time steps and on a spatial resolution of 0.5×0.5 degree (lat/lon). The
152 main processes included are photosynthesis (modelled according to Collatz et al., 1992;
153 Farquhar et al., 1980), auto- and heterotrophic respiration, establishment, mortality, and
154 phenology. For calculating these main processes LPJmL uses climate data (temperature,
155 precipitation, and cloud cover), atmospheric CO₂ concentration, and soil type as input The
156 simulated water fluxes include evaporation, soil moisture, snowmelt, runoff, discharge,
157 interception, and transpiration, which are directly linked to abiotic and biotic properties. In
158 each grid cell LPJmL calculates the performance of nine plant functional types, which
159 represent an assortment of species classified as being functionally similar. In the Amazon
160 basin primarily three of these types are present, namely tropical evergreen and deciduous trees
161 and C4 grasses. In addition to the potential natural vegetation LPJmL can simulate the
162 dynamics of 16 user-defined crops and pasture on area that is not covered by natural
163 vegetation. In analogy to natural vegetation, LPJmL evaluates carbon storage in vegetation,
164 litter and soil as well as water fluxes for these areas. On areas, which are converted to crops
165 and pasture, the vegetation carbon stored in natural vegetation (carbon in living above- and
166 belowground biomass) is removed from the terrestrial domain and added to the litter pool.
167 Due to deforestation, a large amount of carbon is removed from the living biomass, i.e. after
168 some years, the pool size of potential carbon that can be washed out to the river is decreasing
169 dramatically. On the deforested areas growth and harvest of soy bean and managed grasslands
170 is simulated. We distinguished these two types of land use, because soy bean farming and
171 pasture leave different amounts of litter carbon on site. In LPJmL, during soy harvest a
172 maximum of 30% of the aboveground soy biomass, representing the beans, is removed as
173 harvest every year. The remaining aboveground biomass as well as all belowground biomass
174 is left on site and enters the litter pool. Managed grasslands are harvested regularly as well,
175 but always 50% of the aboveground biomass is removed. The remaining aboveground
176 biomass and the total belowground biomass enter the litter pool. Once a stand is harvested the
177 remaining above- and belowground biomass is added to the litter pool. The soil pool remains
178 unchanged. Only after litter decomposition this carbon enters the soil carbon pool. Therefore,
179 after deforestation the amount of carbon washed out from managed land to the river, and
180 entering the riverine carbon system, is much less in size compared to litter exported to the
181 river from undisturbed forests. Changes of soil characteristics and soil carbon pools due to
182 erosion, which is a common consequence of deforestation (Yang et al., 2003) is not included
183 in the model. In summary, the terrestrial ecosystem is losing carbon due to deforestation
184 followed by harvest. Therefore, the riverine ecosystem is receiving less carbon due to reduced
185 terrestrial carbon input after forest was converted to managed land.

186 LPJmL has been shown to reproduce current patterns of biomass production (Cramer et al.,
187 2001; Sitch et al., 2003), carbon emission through fire (Thonicke et al., 2010), also including
188 managed land (Bondeau et al., 2007; Fader et al., 2010; Rost et al., 2008), and water dynamics
189 (Biemans et al., 2009; Gerten et al., 2004, 2008; Gordon et al., 2004; Wagner et al., 2003).
190 The simulated patterns in water fluxes, like evapotranspiration, runoff and soil moisture, are
191 comparable to stand-alone global hydrological models (Biemans et al., 2009; Gerten et al.,
192 2004; Wagner et al., 2003).

193 **2.1.2 RivCM – a riverine carbon model**

194 RivCM is a process-based model that calculates four major ecological processes related to the
195 carbon budget of the Amazon River (Figure 1B). These processes include (1) mobilization,
196 (2) decomposition and (3) respiration within the river, and (4) outgassing of CO₂ to the
197 atmosphere (Langerwisch et al., 2015). During mobilization parts of terrigenous litter and soil
198 carbon, as it is provided by LPJmL, is imported to the river, depending on inundated area. The
199 further processing of the terrigenous carbon in the river happens during its decomposition,
200 which represents the manual breakup, and its respiration, representing the biochemical
201 breakup. Finally the CO₂ that is produced during respiration can outgas if the saturation
202 concentration is exceeded (Langerwisch et al., 2015). These four processes directly control
203 the most relevant riverine carbon pools, namely particulate organic carbon (POC), dissolved
204 organic carbon (DOC), and inorganic carbon (IC), as well as outgassed atmospheric carbon
205 (representing CO₂), and exported riverine carbon to the ocean (either as POC, DOC, or IC).

206 The model is coupled to LPJmL by using the calculated monthly litter and soil carbon and
207 water amounts as inputs. It operates at the spatial resolution of 0.5 × 0.5 degree (lat/lon) and
208 on monthly time steps. The ability of the coupled model LPJmL-RivCM to reproduce current
209 conditions in riverine carbon concentration and export to either the atmosphere or the ocean
210 has been shown and discussed by Langerwisch et al. (2015). A validation of the carbon pools
211 and fluxes with observed data shows that RivCM produces results that are within the range of
212 observed concentrations of both organic and inorganic carbon pools. Model results strongly
213 underestimate the amount of outgassed carbon while the carbon discharged to the ocean is
214 overestimated. There are still large uncertainties in the process understanding of riverine carbon
215 processes that translates to uncertainty in the parameter estimation. Therefore, a respective model
216 like we have applied here can currently only reproduce broad estimations of exported CO₂
217 (outgassing) and exported organic carbon (discharge). In general the model reaction to climate
218 change alone and in combination with deforestation and land-use change is as expected (e.g.
219 reduction of organic carbon due to deforestation, increase of inorganic carbon due to climate
220 change). Therefore, we think it is reasonable to use our model to estimate changes in process
221 relations and general trends. Further data-model comparison and improved parameterization are
222 still required to allow assessing the simulated absolute numbers. Despite these shortcomings we
223 make use of the coupled model system of LPJmL and RivCM to assess the combined impacts
224 of climate change and deforestation.

225 2.2 Model simulation

226 All transient LPJmL runs were preceded by a 1000-year spin-up during which the pre-
227 industrial CO₂ level of 280 ppm and the climate of the years 1901-1930 have been repeated to
228 obtain equilibria for vegetation, carbon, and water pools. All transient runs of the coupled
229 model LPJmL-RivCM have been preceded by a 90-years-spinup during which the climate and
230 CO₂ levels of 1901-1930 have been repeated to obtain equilibria for riverine carbon pools.

231 LPJmL-RivCM was run on a 0.5° × 0.5° degree (lat/lon) spatial resolution for the years 1901
232 to 2099. For the estimation of the impact of projected climate change (CC) and deforestation
233 (Defor), simulations have been conducted driven by five General Circulation Models
234 (GCMs), each calculated for three SRES emission scenarios, and three LUC scenarios.

235 2.2.1 Climate change and deforestation data sets

236 To assess the effect of future climate change, projections of five GCMs (see also Jupp et al.,
237 2010; Randall et al., 2007), using three SRES scenarios (A1B, A2, B1) (Nakićenović et al.,
238 2000) have been applied (Figure 1A). The GCMs, namely MIUB-ECHO-G, MPI-ECHAM5,
239 MRI-CGCM2.3.2a, NCAR-CCSM3.0, UKMO-HadCM3, cover a wide range in terms of
240 temperature and precipitation and have therefore been chosen to account for uncertainty in
241 climate projections. The emission scenario SRES A1B describes a development of very rapid
242 economic growth with convergence among regions, and a balanced future energy source
243 between fossil and non-fossil. SRES A2 describes a development of a very heterogeneous
244 world with slow economic growth. And SRES B1 describes a development of converging
245 world similar to A1B but with more emphasis on service and information economy.

246 To estimate the additional effects of deforestation on riverine carbon pools and fluxes three
247 land use scenarios were applied: two scenarios directly relate to different intensity of
248 deforestation, and one represents a reference scenario with complete coverage by natural
249 vegetation (NatVeg scenario, hereafter). The two deforestation scenarios are based on the
250 SimAmazonia projections (Soares-Filho et al., 2006, see also Figure 2). The authors estimate
251 the development of deforestation in the Amazon basin until 2050 based on historical trends
252 and projected developments. In the business-as-usual scenario (BAU) they assume that recent
253 deforestation trends continue, the number of paved highways increases, and new protected
254 areas are not established. In contrast, deforestation is more efficiently controlled in the
255 governance scenario (GOV). For this scenario the authors assume that the Brazilian
256 environmental legislation is implemented across the Amazon basin and the size of the area
257 under the *Protected Areas Program* increases. The SimAmazonia scenarios cover the years
258 from 2001 to 2050. After 2050 the fraction of deforested area is kept constant. From 2051
259 until the end of the century the only driver of change is the continuing climate change. This
260 approach enables us to estimate the consequences of combined dynamics of deforestation and
261 climate change until 2050 and the effects of intensified climate change after 2050, when
262 deforestation is halted at its maximum. Deforestation rates preceding the scenarios (before
263 2001) were derived from extrapolating the data into the past. LPJmL requires historic land-
264 cover information to correctly capture transient carbon dynamics. The model starts to simulate
265 vegetation dynamics from bare ground and can't be initialized with a land-cover map of a

266 particulate year. It was therefore necessary to develop an approach which produced consistent
 267 land-cover information for the (undisturbed) past and the deforestation scenarios. For that, the
 268 mean annual rate of deforestation was calculated for the reference period of 2001 to 2005 (Eq.
 269 (1)) and this rate was applied to calculate the fraction of deforested area F_t for the years 1901
 270 to 2000 for each cell (Eq. (2)).

$$r = \left(\sum_{t=2001}^{2005} \frac{F_t}{F_{t+1}} \right) \times \frac{1}{2006 - 2001} \quad (1)$$

$$F_t = F_{2001} \times r^{2001-t} \quad (2)$$

271

272 To evaluated spatial differences in the basin we defined three sub-regions (see Table 1). Three
 273 regions were selected for further detailed analysis and differ in projected changes in
 274 inundation patterns and in deforestation intensity. R1 is located in the Western basin with
 275 projected increase in inundation length and inundated area (Langerwisch et al., 2013)
 276 combined with low land use intensity. R2 is a region covering the Amazon main stem with
 277 intermediate changes in inundation (Langerwisch et al., 2013) and intermediate land use
 278 intensity. And R3 is a region with projected decrease in duration of inundation and inundated
 279 area (Langerwisch et al., 2013) combined with high land use intensity. In the deforestation
 280 scenarios we assume that on 15% of the deforested area soy bean is grown and 85% of the
 281 area is used as pasture for beef production (Costa et al., 2007).

282 **2.3 Analysis of simulation results**

283 The separate effect of deforestation (E_{Defor}) is estimated by calculating the differences
 284 between future carbon amounts (2070-2099) produced in the deforestation scenarios (GOV or
 285 BAU) and future carbon amounts produced in the potential natural vegetation scenario
 286 (NatVeg), where no deforestation is assumed. The combined effect of climate change and
 287 deforestation ($E_{CCDefor}$) is estimated by calculating the differences between future carbon
 288 amounts produced in the deforestation scenarios and reference carbon amounts (1971-2000)
 289 produced in the NatVeg scenario. We analysed all four riverine carbon pools (riverine
 290 particulate organic carbon (POC), dissolved organic carbon (DOC), riverine inorganic carbon
 291 (IC) and outgassed carbon). The relative changes in POC and DOC show similar patterns (see
 292 Figure S1), therefore exemplary POC is shown and discussed in detail.

293 **2.3.1 Evaluation of potential future changes**

294 Spatial effects of the two deforestation scenarios (GOV and BAU) on the different riverine
 295 carbon pools and fluxes have been estimated by calculating the common logarithm (\log_{10}) of
 296 the ratio of mean future (2070-2099) carbon amounts of the deforestation scenarios and mean
 297 future carbon amounts of the NatVeg scenario (E_{Defor} , Eq. (3)) for each simulation run.

$$E_{Defor} = \log_{10} \frac{\sum_{t=2070}^{2099} C_{Defor_t}}{\sum_{t=2070}^{2099} C_{NatVeg_t}} \quad (3)$$

298 To estimate changes caused by the combination of climate change and deforestation $E_{CCDefor}$
 299 compares future carbon pools in the deforestation scenarios to carbon pools during the
 300 reference period (1971-2000) in the NatVeg scenario (Eq. (4)).

$$E_{CCDefor} = \log_{10} \frac{\sum_{t1=2070}^{2099} C_{Defor_{t1}}}{\sum_{t2=1971}^{2000} C_{NatVeg_{t2}}} \quad (4)$$

301 Each simulation run combines deforestation and emission scenarios and aggregates the
 302 outputs for all five climate model inputs used. To identify areas where the differences
 303 between values in the reference period and future values are significant (p-value <0.05), the
 304 Wilcoxon Rank Sum Test for not-normally distributed datasets (Bauer, 1972) has been
 305 applied for each cell.

306 Additionally to the spatial assessment, time series were deduced based on mean values over
 307 the entire basin and each of the three exemplary regions R1, R2 and R3. These means of the
 308 carbon pools were calculated for every year during the simulation period. Changes have been
 309 expressed as the five-year-running-mean of the quotient of annual future carbon amounts in
 310 the deforestation and in the NatVeg scenarios. These analyses have been conducted both for
 311 the whole Amazon basin and for three selected sub-regions.

312 2.3.2 Estimating the dominant driver for changes

313 We estimated which factor is causing the observed changes the most. To estimate the
 314 contribution of either climate change (D_{CC} , Eq. (5)) or deforestation (D_{Defor} , Eq. (6)),
 315 reference carbon amounts of the NatVeg scenario have been compared to future amounts of
 316 the NatVeg scenario (D_{CC}), and future carbon amounts of the NatVeg scenario have been
 317 compared to future amounts of the deforestation scenarios (D_{Defor}).

$$D_{CC} = \left| \log_{10} \frac{\sum_{t1=2070}^{2099} C_{NatVeg_{t1}}}{\sum_{t2=1971}^{2000} C_{NatVeg_{t2}}} \right| \quad (5)$$

$$D_{Defor} = |E_{Defor}| \quad (6)$$

318 We define a cell as dominated by climate change effects, if $D_{CC} > D_{Defor}$ and dominated by
 319 deforestation effects if $D_{CC} < D_{Defor}$. The impact values D_{CC} and D_{Defor} ($median_{POC} = 0.9695$,
 320 $median_{IC} = 1.0106$, and $median_{outgassedC} = 0.9982$) have been rounded to the second decimal
 321 place. If both values are equal, the two effects balance each other.

322

323 3 Results

324 3.1 Changes caused by deforestation

325 Deforestation decreases riverine particulate and dissolved organic carbon (POC and DOC).
326 When continuing high deforestation rates as projected under the BAU deforestation scenario,
327 the decrease in POC is more intense than under GOV deforestation rates (Figure 3A and
328 Figure 3B; for DOC see Figures. S1A and S1B). In some highly deforested sites in the South-
329 East of the basin the amount of POC is only 10% of the amount under no deforestation
330 (indicated by E_{Defor}). This pattern is robust between the model realizations with a high
331 agreement of the results amongst the five climate models. In the deforestation scenarios the
332 changes in future POC are drastic, even though the difference between the three emission
333 scenarios A1B, A2, and B1 are very small. However, in some regions within the Amazon
334 basin POC increases (up to 3fold), especially in mountain regions (e.g. Andes and Guiana
335 Shield). Although POC and DOC respond similar in relative terms (see Figure S1), the
336 absolute amounts are approximately twice as high for DOC compared to POC (Table 2). The
337 mean basin-wide loss in POC ranges between $0.13 \times 10^{12} \text{ g yr}^{-1}$ (A2) and $0.24 \times 10^{12} \text{ g yr}^{-1}$
338 (A1B) in the GOV scenario, and between $0.37 \times 10^{12} \text{ g yr}^{-1}$ (A2) and $0.48 \times 10^{12} \text{ g yr}^{-1}$ (A1B) in
339 the BAU scenario. The SRES A2 scenario causes the largest changes in POC, further
340 increasing the loss caused by deforestation.

341 Changes in outgassed riverine carbon caused by deforestation (Figure 3C and Figure 3D)
342 show a similar pattern as the changes in POC, with an even clearer effect of deforestation on a
343 larger area. In both scenarios deforestation decreases outgassed carbon to up to one tenth
344 compared to the amount produced under the NatVeg scenario. The agreement between the
345 five climate models is even larger than in POC. In contrast to the overall pattern, some areas
346 in the Andes and the Guiana Shield show an increase in outgassed carbon of up to a factor of
347 30, but these areas are an exception. Like in POC the differences between the SRES scenarios
348 are only minor. For the absolute values see Table 2.

349 For riverine inorganic carbon (IC) deforestation caused significant changes (E_{Defor} , p-value
350 < 0.05) only in small areas (Figure 3E and Figure 3F). In these regions, in the very South of
351 the basin and in single spots in the North, i.e. in the headwaters of the watershed, IC increases
352 by a factor of up to 1.2. Besides these areas of increase, a slight decrease of about 5% is
353 simulated for the region along the main stem of the Amazon River, downstream of Manaus
354 and along the Rio Madeira and the Rio Tapajós. In contrast to POC, the spatial pattern of
355 change in IC does not obviously follow the deforestation patterns. Therefore, the differences
356 between the two deforestation scenarios GOV and BAU scenarios are minor. Whereas POC,
357 DOC, and outgassed carbon show a clear decrease due to deforestation, IC shows a nearly
358 neutral response with maximal mean basin-wide gains (for absolute values see Table 2).

359 3.2 Changes caused by a combination of deforestation and climate change

360 Climate change and deforestation together will lead to large overall changes in the amount of
361 riverine and exported carbon. Riverine POC and DOC amounts will decrease by about 19.8%
362 and 22.2%, respectively, and exported organic carbon will decrease by about 38.1% (Figure

363 5). In contrast riverine IC will increase by about 100%, combined with a slight increase of
364 outgassed carbon by about 2.7% (Figure 5). In detail, the basin-wide changes in the amount of
365 POC (Figure 5A-B and Figure S2) caused by deforestation and climate change range between
366 a 2.5-fold increase and a decrease to one tenth. The increase is mainly caused by climate
367 change (indicated as blue area in the inset in Figure 5), whereas the decrease is mainly caused
368 by deforestation (red area in inset). The differences mainly induced by deforestation are larger
369 in the BAU compared to the GOV scenario. In contrast, the differences caused by climate
370 change show no large differences between the two deforestation scenarios. The differences
371 between the emission scenarios are minor (see also Table 2). In some areas the dominance of
372 forcing shifts from climate change dominance (D_{CC}) for the GOV scenario (green cell border)
373 to deforestation dominance (D_{Defor}) for the BAU scenario (red cell border) due to the higher
374 land use intensity as a result of deforestation (see also Table 3). While in the GOV scenario
375 20% of all cells are dominated by deforestation impacts, this value increases for the BAU
376 scenario to 30%. During the first decades (2000-2030) basin-wide POC is partly larger in the
377 deforestation scenarios than in the NatVeg scenario by up to 2% in 2000 and about 1% in
378 2020 (Figure 6A). All climate models show reduced POC amounts in the deforestation
379 scenarios compared to the NatVeg scenario after 2040. The POC amount in the GOV
380 deforestation scenario decreases gradually until the decrease levels off in the late 2060s, i.e.
381 ten years after the constant deforestation area is kept constant. In the BAU scenario, POC
382 decreases strongly in the 2040 to 2060s leading to a loss of about 25% compared to 10% in
383 the GOV scenario. In addition to Figure 6, which shows the temporal development under
384 deforestation only, we provide Figure S2, which shows the developments taking the
385 combination of deforestation and climate change into account.

386 The three sub-regions R1 to R3 show different patterns (Figure 6A). While in region R1 the
387 difference in the POC amounts between the GOV and the BAU scenario is only small,
388 reflecting the low deforestation in this region, the differences between the two deforestation
389 scenarios are more explicit in regions R2 and especially in R3 (with the largest area
390 deforested), where in addition model uncertainty is low. Starting in the 2050s, the variation
391 between different emission scenarios and climate models increases. Alike the results of the
392 impact of deforestation alone POC and DOC show a similar pattern (see also Table 2).

393 The changes in outgassed carbon (Figure 5C-D and Figure 6B) are in the same range as
394 changes in POC. Climate change increases outgassed carbon by about 20%, especially in the
395 North-Western basin (Figure 5C-D). The deforestation induces a decrease on outgassed
396 carbon to one tenth in areas with high fraction of deforested area, i.e. in the Eastern and
397 South-Eastern basin. Again, the differences in effects are much larger between the two
398 deforestation scenarios (GOV vs. BAU) than between the different emission scenarios (see
399 also Table 2). After 2050 the rate of deforestation determines the differences in the amount of
400 outgassed carbon (Figure 6B) as well. The outgassed carbon directly depends on the available
401 POC, therefore the time series of both, POC and IC widely match. Under the GOV scenario
402 the basin-wide loss of outgassed carbon is about 16% towards the end of the century. The
403 results of the BAU scenario show an average loss of outgassed carbon of 28%.

404 Changes in inorganic carbon (IC) are mainly driven by climate change (under all emission
405 scenarios) and less by the magnitude of deforestation (Figure 5E-F and Figure 6C, Tables 2

406 and 3). In about half of the Amazon basin the IC amount significantly changes due to climate
407 change (insignificant changes in the other 50%), but in no cell due to deforestation. The
408 magnitude of change varies between emission scenarios: the increase in IC is up to 4-fold in
409 the A2 scenario and up to 2.5-fold in the B1 scenario (see Table 2). For both deforestation
410 scenarios the gain of IC is dominant until 2050, while the basin-wide trend becomes unclear
411 afterwards. However, sub-regions like R1 and R3 show a slight increase during the whole
412 century (Figure 6F,J,M).

413

414 **4 Discussion**

415 Deforestation is, besides climate change, the largest threat to Amazonia. It leads directly to a
416 decrease in terrestrial biomass and an increase in CO₂ emissions (Potter et al., 2009) and has
417 indirect effects on aquatic biomass, diversity of species and their habitats and the climate
418 (Asner and Alencar, 2010; Bernardes et al., 2004; Costa et al., 2003). Our results show that
419 deforestation is also likely to change the amount of riverine organic carbon as well as
420 exported carbon.

421 We identified a basin-wide reduction in riverine particulate and dissolved organic carbon
422 pools by about 10% to 25% by the end of this century (Figure 3 and Figure 6). This reduction
423 is particularly pronounced in areas of high deforestation intensity along the *Arc of*
424 *Deforestation*, at the Rio Madeira and the last 500 km stretch of the Rio Amazon, where large
425 deforestation rates reduce terrestrial carbon storage. In the first decades of the 21st century the
426 differences in carbon amounts between the two deforestation scenarios are only small (Figure
427 6). During these decades the deforestation-induced increase in discharge is able to partly
428 offset the decreasing amount of terrigenous organic matter which is the source of riverine
429 organic matter. In the model, the increase of discharge after deforestation is caused by a less
430 intense use of the available (soil) water by the crops, as compared to natural vegetation, which
431 leaves more water for discharge (as also reported by Costa et al., 2003). After the 2050s, the
432 differences in the organic carbon pools caused by deforestation become more obvious (Figure
433 6), with larger carbon decrease under the more severe BAU scenario. The same patterns occur
434 in the two regions with the pronounced deforestation (R1 and R2). Here the reduction of
435 terrestrial carbon directly reduces the amount of riverine carbon. The variation in future
436 riverine carbon fluxes within each deforestation scenario can be attributed to the differences
437 climate projections and emission scenarios, especially after 2060 when deforested area
438 remains constant and the lagged deforestation effects vanish. In regions with low
439 deforestation intensity (i.e. R1) the effects of land use change are much smaller and the
440 climate change effects dominate the change in riverine organic carbon and outgassed carbon.
441 Under the GOV scenario litter is constantly provided by the natural vegetation and small scale
442 deforestation, and therefore fills up the litter and soil carbon pools, which are responsible for
443 the POC and the outgassed carbon. There is a much clearer drop in the BAU scenario, where a
444 larger fraction of the cell is subject to deforestation; partly 100% of the cell area is deforested
445 in this scenario. In areas where the drop already starts before 2050 (e.g. Figure 6K and L,
446 showing the results for R3) the deforestation in parts of the area already reached 100% before

447 2050 (also compare with timelines in Figure 2B). In these cells there is a drastically reduced
448 influx of carbon to the litter pool (only from crops) and therefore we already see the drop
449 earlier than in other areas (e.g. R1).

450 The reduction in the riverine organic carbon pools will have consequences for the floodplain
451 and the river itself. Floodplains as well as riverine biotopes depend on the annually recurring
452 input of organic material, either as food supply or fertilizer (Junk and Wantzen, 2004). The
453 productivity of the floodplain forests is mainly driven by the input of nutrients which are
454 basically sediments and organic material (Worbes, 1997). While the sediment input (also
455 adding nutrients) might increase due to increased discharge, the input of organic material
456 from upstream areas will decrease, leading to a reduced terrestrial and riverine productivity.
457 This reduced productivity will certainly impact many animal species that rely on the food
458 supplied by trees, such as fruits or leaves. The reduced supply of fertilizer and food will
459 therefore likely affect plant and animal species compositions on local and regional scales
460 (Junk and Wantzen, 2004; Worbes, 1997).

461 Additionally, deforestation will have secondary effects, including a reduction in evasion of
462 CO₂ from the water (outgassed carbon). Lower terrestrial productivity after deforestation
463 decreases the organic carbon material in the river and thus also the respiration to CO₂. This is
464 opposed by the higher respiration rate as a result of increased temperatures due to climate
465 change. These indirect effects of deforestation on riverine carbon dynamics have to be
466 included in future carbon balance estimates of the sink/source behaviour of the Amazon basin,
467 since it directly couples the change in land use to the atmospheric, marine and therefore
468 global carbon fluxes.

469 In contrast to the amount of riverine organic carbon and outgassed carbon the amount of
470 riverine inorganic carbon does not show a significant effect of deforestation. The inorganic
471 carbon in the water is only marginally affected by deforestation because the amount of IC that
472 remains in the water depends on the saturation of the water with of IC, which is calculated
473 depending on the water temperature and the atmospheric CO₂ concentration. Climate change-
474 induced higher water temperature causes a reduction in solubility of CO₂, and higher
475 atmospheric CO₂ concentrations lead to an increase in dissolved CO₂. The combination of
476 both effects leads to a slight increase in dissolved inorganic carbon in the beginning and a
477 neutral signal towards the end of the century independently of the deforestation. Any changes
478 in the amount of IC can either be attributed to climate change (increasing temperatures and
479 atmospheric CO₂ concentration) or – to a much smaller extent – to changes in the water
480 amount in the cell. The latter can be an effect of deforestation as it is known that deforestation
481 alters the discharge (Costa et al., 2003).

482 The deforestation of tropical forests will not only affect processes within the rainforest, but
483 also processes in the adjacent Atlantic Ocean. Currently, the annual export of about 6,300 km³
484 of freshwater is accompanied by 40×10¹² g of organic carbon to the Atlantic Ocean
485 (Gaillardet et al., 1997; Moreira-Turcq et al., 2003). The present study shows that
486 deforestation leads to a reduction in the exported organic carbon to the ocean by
487 approximately 40%. In the NatVeg scenario the proportion of exported organic carbon to the
488 ocean makes up about 0.8-0.9% of the net primary production (NPP), whereas in the heavily

489 deforested BAU scenario this proportion is reduced to about 0.5-0.6%. The reduction in the
490 ratio of exported carbon to NPP by deforestation indicates a less pronounced future sink, since
491 the organic carbon is directly extracted from the forest and additionally indirectly from the
492 ocean. The Amazon basin is considered a carbon sink (Lewis et al., 2011). In central
493 Amazonia net primary production sums up to about 1×10^9 g C km⁻² yr⁻¹ (Malhi et al., 2009).
494 Earlier results showed that climate change alone will increase the amount of outgassed carbon
495 from the Amazon basin by about 40%, while the export to the Atlantic Ocean remains nearly
496 unchanged (Langerwisch et al., 2016). Our results show that additional deforestation will
497 offset the trend in outgassed carbon (only +3%), but will have larger effects on the export to
498 the ocean (-38%). Therefore, future assessments of climate-change and deforestation-induced
499 changes on the carbon balance of the Amazon basin have to include the amount of carbon
500 exported to the ocean and outgassed from the river basin to the atmosphere.

501 The import of organic material to the ocean positively impacts the respiration and production
502 of the Atlantic Ocean off the coast of South America (Körtzinger, 2003; Cooley and Yager,
503 2006; Cooley et al., 2007; Subramaniam et al., 2008). A reduction of the import might
504 therefore reduce the productivity in the coast-near ocean since these coastal zones depend on
505 the imported organic matter (Cooley and Yager, 2006; Körtzinger, 2003; Subramaniam et al.,
506 2008) and might have further impacts along the trophic cascade including herbivorous and
507 piscivorous fish. Besides the reduced organic carbon, higher amounts of nutrients may be
508 imported to the ocean, because the nutrients are only marginally taken up within the river and
509 by the former intact adjacent forests. The imports of both, less organic carbon and more
510 nutrients, might induce changes in oceanic heterotrophy and primary production.

511

512 **4.1 Shortcomings of the approach**

513 The strong decrease of organic carbon may be overestimated because of our model
514 assumptions, which include a complete removal of the natural vegetation carbon during
515 deforestation (see e.g. Figure 6). In reality, the complete conversion of the floodplain forests
516 to cropland or pasture is not very likely. In the more severe deforestation scenario (BAU)
517 about 6% of the area is deforested (Soares-Filho et al., 2006). In our scenarios this also
518 includes areas which are temporarily flooded. Since temporarily inundated areas cannot be
519 easily converted to agricultural area or settlements, this might lead to an overestimation of
520 deforested area. But, for example in Manaus, floodplains within a radius of about 500 km
521 around the city have been extensively logged for construction purposes between 1960 and
522 1980 (Goulding et al., 2003).

523 In our study deforestation is simulated by partial or complete removal of vegetation carbon.
524 This also reduces the litter and soil carbon through respiration over time, since these carbon
525 pools are reduced in size since less dead organic material generated by the crops and managed
526 land remains on site, other is harvested. Therefore, our estimates represent more drastic
527 changes in riverine carbon dynamics. The sharp decrease in POC and outgassed carbon after
528 2050, as it is one result of our study, is caused by the implementation of carbon removal in the
529 model. During inundation the cells are partly or completely covered with water, which leads

530 to the export of organic material. After the gradual decrease of forest cover (and therewith
531 input of organic material) before 2050, there is a depletion of the remaining organic material
532 in the following years. By a more gradual implementation of inundation in the model this
533 harsh decrease would be softened.

534 In this study the mobilization of terrigenous organic material is exclusively controlled by
535 inundation. A model that also considers the impact of precipitation, vegetation cover and
536 slope on erosion would likely lead to an increase in erosion and thus to the import of organic
537 matter to the river (McClain and Elsenbeer, 2001) in the first years after deforestation.
538 However, this additional influx of carbon would only be temporal, since the soil and litter
539 carbon pools would be eroded after some years (McClain and Elsenbeer, 2001). Thus, we
540 assume that for the investigation of the long-term dynamics of carbon pools and fluxes, such
541 erosion effects are only of minor importance.

542

543 **5 Conclusion**

544 Deforestation decreases terrestrial biomass and contributes to a further increase in CO₂
545 emissions, which reduces the terrestrial carbon sequestration potential (Houghton et al., 2000;
546 Potter et al., 2009). Moreover, our results show that deforestation will lead to a significant
547 decrease of exported terrigenous organic carbon, leading to a reduction of the amount of
548 riverine organic carbon. The climate change effects additionally increase in the amount of
549 riverine inorganic carbon. Deforestation further decreases the amount of riverine organic
550 carbon leading to a combined decrease by about 20% compared to 10% under climate change
551 alone (Langerwisch et al. 2015). While climate change alone leaves the export to the Atlantic
552 Ocean with +1% nearly unchanged (Langerwisch et al. 2015), considering deforestation will
553 now decrease the export of organic carbon to the ocean by about 40%. In contrast climate
554 change will strongly increase the outgassed carbon by about 40% (Langerwisch et al. 2015),
555 but including deforestation will reduce this increase to only +3%.

556 These changes in the hydrological regimes and the fluvial carbon pools might add to the
557 pressures that are being imposed on the Amazon ecosystems (Asner et al., 2006; Asner and
558 Alencar, 2010), with strong consequences for ecosystem stability (Brown and Lugo, 1990;
559 Foley et al., 2002; von Randow et al., 2004). For instance, fish play a key role in seed
560 dispersal along the Amazon. If floodplains turn into less productive grounds for juvenile fish,
561 these changes might have considerable effects on local vegetation recruitment dynamics and
562 regional plant biodiversity (Horn et al., 2011). We therefore strongly advocate the combined
563 terrestrial and fluvial perspective of our approach, and its ability to address both climate and
564 land use change.

565

566 *Acknowledgements.* We thank “Pakt für Forschung der Leibniz-Gemeinschaft” for funding the
567 TRACES project for FL. AR was funded by FP7 AMAZALERT (Project ID 282664) and
568 Helmholtz Alliance ‘Remote Sensing and Earth System Dynamics’. We also thank Susanne

569 Rolinski and Dieter Gerten for discussing the hydrological aspects. We thank Alice Boit for
570 fruitful comments on the manuscript. Additionally we thank our LPJmL and ECOSTAB
571 colleagues at PIK for helpful comments on the design of the study and the manuscript. We
572 also thank the anonymous reviewers and the handling editor whose comments and
573 suggestions greatly improved the manuscript.

574 *Author contributions.* Model development: FL, BT, WC. Data analysis: FL, AR, KT. Drafting
575 the article: FL, AW, BT, AR, KT.

576

577 **6 References**

578 Aguiar, A. P. D., Vieira, I. C. G., Assis, T. O., Dalla-Nora, E. L., Toledo, P. M., Oliveira
579 Santos-Junior, R. A., Batistella, M., Coelho, A. S., Savaget, E. K., Aragão, L. E. O. C., Nobre,
580 C. A. and Ometto, J. P. H.: Land use change emission scenarios: anticipating a forest
581 transition process in the Brazilian Amazon, *Global Change Biology*, 22(5), 1821–1840,
582 doi:10.1111/gcb.13134, 2016.

583 Anderson, J. T., Nuttle, T., Saldaña Rojas, J. S., Pendergast, T. H. and Flecker, A. S.:
584 Extremely long-distance seed dispersal by an overfished Amazonian frugivore, *Proceedings*
585 *of the Royal Society B: Biological Sciences*, 278, 3329–3335, doi:10.1098/rspb.2011.0155,
586 2011.

587 Asner, G. P. and Alencar, A.: Drought impacts on the Amazon forest: the remote sensing
588 perspective, *New Phytologist*, 187(3), 569–578, doi:10.1111/j.1469-8137.2010.03310.x,
589 2010.

590 Asner, G. P., Broadbent, E. N., Oliveira, P. J. C., Keller, M., Knapp, D. E. and Silva, J. N. M.:
591 Condition and fate of logged forests in the Brazilian Amazon, *Proceedings of the National*
592 *Academy of Sciences*, 103(34), 12947–12950, 2006.

593 Bauer, D. F.: Constructing confidence sets using rank statistics, *Journal of the American*
594 *Statistical Association*, 67(339), 687–690, 1972.

595 Bernardes, M. C., Martinelli, L. A., Krusche, A. V., Gudeman, J., Moreira, M., Victoria, R.
596 L., Ometto, J. P. H. B., Ballester, M. V. R., Aufdenkampe, A. K., Richey, J. E. and Hedges, J.
597 I.: Riverine organic matter composition as a function of land use changes, *Southwest*
598 *Amazon, Ecological Applications*, 14(4), S263–S279, doi:10.1890/01-6028, 2004.

599 Biemans, H., Hutjes, R. W. A., Kabat, P., Strengers, B. J., Gerten, D. and Rost, S.: Effects of
600 precipitation uncertainty on discharge calculations for main river basins, *Journal of*
601 *Hydrometeorology*, 10(4), 1011–1025, doi:10.1175/2008jhm1067.1, 2009.

602 Bondeau, A., Smith, P. C., Zaehle, S., Schaphoff, S., Lucht, W., Cramer, W., Gerten, D.,
603 Lotze-Campen, H., Müller, C., Reichstein, M. and Smith, B.: Modelling the role of agriculture
604 for the 20th century global terrestrial carbon balance, *Global Change Biology*, 13(3), 679–
605 706, doi:10.1111/j.1365-2486.2006.01305.x, 2007.

606 Brown, S. and Lugo, A. E.: Tropical secondary forests, *Journal of Tropical Ecology*, 6(1), 1–
607 32, 1990.

- 608 Collatz, G. J., Ribas-Carbo, M. and Berry, J. A.: Coupled photosynthesis-stomatal
609 conductance model for leaves of C4 plants, *Functional Plant Biology*, 19(5), 519–538,
610 doi:10.1071/PP9920519, 1992.
- 611 Cooley, S. R. and Yager, P. L.: Physical and biological contributions to the western tropical
612 North Atlantic Ocean carbon sink formed by the Amazon River plume, *Journal of*
613 *Geophysical Research-Oceans*, 111(C08018), doi:10.1029/2005JC002954, 2006.
- 614 Cooley, S. R., Coles, V. J., Subramaniam, A. and Yager, P. L.: Seasonal variations in the
615 Amazon plume-related atmospheric carbon sink, *Global Biogeochemical Cycles*, 21(3),
616 doi:10.1029/2006GB002831, 2007.
- 617 Costa, M. H., Botta, A. and Cardille, J. A.: Effects of large-scale changes in land cover on the
618 discharge of the Tocantins River, Southeastern Amazonia, *Journal of Hydrology*, 283(1–4),
619 206–217, doi:10.1016/S0022-1694(03)00267-1, 2003.
- 620 Costa, M. H., Yanagi, S. N. M., Souza, P., Ribeiro, A. and Rocha, E. J. P.: Climate change in
621 Amazonia caused by soybean cropland expansion, as compared to caused by pastureland
622 expansion, *Geophysical Research Letters*, 34(7), doi:10.1029/2007GL029271, 2007.
- 623 Cramer, W., Bondeau, A., Woodward, F. I., Prentice, I. C., Betts, R. A., Brovkin, V., Cox, P.
624 M., Fisher, V., Foley, J. A., Friend, A. D., Kucharik, C., Lomas, M. R., Ramankutty, N.,
625 Sitch, S., Smith, B., White, A. and Young-Molling, C.: Global response of terrestrial
626 ecosystem structure and function to CO₂ and climate change: results from six dynamic global
627 vegetation models, *Global Change Biology*, 7(4), 357–373, 2001.
- 628 Eva, H. D., Belward, A. S., De Miranda, E. E., Di Bella, C. M., Gond, V., Huber, O., Jones,
629 S., Sgrenzaroli, M. and Fritz, S.: A land cover map of South America, *Global Change*
630 *Biology*, 10(5), 731–744, 2004.
- 631 Fader, M., Rost, S., Müller, C., Bondeau, A. and Gerten, D.: Virtual water content of
632 temperate cereals and maize: Present and potential future patterns, *Journal of Hydrology*,
633 384(3–4), 218–231, doi:10.1016/j.jhydrol.2009.12.011, 2010.
- 634 Farquhar, G. D., van Caemmerer, S. and Berry, J. A.: A biochemical model of photosynthetic
635 CO₂ assimilation in leaves of C3 species, *Planta*, 149, 78–90, 1980.
- 636 Fearnside, P. M.: Environment: Deforestation soars in the Amazon, *Nature*, 521(7553), 423–
637 423, doi:10.1038/521423b, 2015.
- 638 Foley, J. A., Botta, A., Coe, M. T. and Costa, M. H.: El Niño-Southern Oscillation and the
639 climate, ecosystems and rivers of Amazonia, *Global Biogeochemical Cycles*, 16(4), 79/1-
640 79/17, doi:10.1029/2002GB001872, 2002.
- 641 Foley, J. A., Asner, G. P., Costa, M. H., Coe, M. T., DeFries, R., Gibbs, H. K., Howard, E. A.,
642 Olson, S., Patz, J., Ramankutty, N. and Snyder, P.: Amazonia revealed: forest degradation and
643 loss of ecosystem goods and services in the Amazon Basin, *Frontiers in Ecology and the*
644 *Environment*, 5(1), 25–32, doi:10.1890/1540-9295(2007)5[25:ARFDAL]2.0.CO;2, 2007.
- 645 Gaillardet, J., Dupré, B., Allègre, C. J. and Négrel, P.: Chemical and physical denudation in
646 the Amazon River basin, *Chemical Geology*, 142(3–4), 141–173, 1997.

- 647 Gerten, D., Schaphoff, S., Haberlandt, U., Lucht, W. and Sitch, S.: Terrestrial vegetation and
648 water balance - hydrological evaluation of a dynamic global vegetation model, *Journal of*
649 *Hydrology*, 286(1–4), 249–270, doi:10.1016/j.jhydrol.2003.09.029, 2004.
- 650 Gerten, D., Rost, S., von Bloh, W. and Lucht, W.: Causes of change in 20th century global
651 river discharge, *Geophysical Research Letters*, 35(20), doi:L20405 10.1029/2008gl035258,
652 2008.
- 653 Godar, J., Gardner, T. A., Tizado, E. J. and Pacheco, P.: Actor-specific contributions to the
654 deforestation slowdown in the Brazilian Amazon, *Proceedings of the National Academy of*
655 *Sciences*, 111(43), 15591–15596, doi:10.1073/pnas.1322825111, 2014.
- 656 Gordon, W. S., Famiglietti, J. S., Fowler, N. L., Kittel, T. G. F. and Hibbard, K. A.:
657 Validation of simulated runoff from six terrestrial ecosystem models: results from VEMAP,
658 *Ecological Applications*, 14(2), 527–545, doi:10.1890/02-5287, 2004.
- 659 Goulding, M., Barthem, R. and Ferreira, E.: *The Smithsonian Atlas of the Amazon*,
660 *Smithsonian*, Washington and London., 2003.
- 661 Hamilton, S. K.: Biogeochemical implications of climate change for tropical rivers and
662 floodplains, *Hydrobiologia*, 657(1), 19–35, doi:10.1007/s10750-009-0086-1, 2010.
- 663 Hedges, J. I., Mayorga, E., Tsamakis, E., McClain, M. E., Aufdenkampe, A., Quay, P.,
664 Richey, J. E., Benner, R., Opsahl, S., Black, B., Pimentel, T., Quintanilla, J. and Maurice, L.:
665 Organic matter in Bolivian tributaries of the Amazon River: A comparison to the lower
666 mainstream, *Limnology and Oceanography*, 45(7), 1449–1466, 2000.
- 667 Hoorn, C., Wesselingh, F. P., ter Steege, H., Bermudez, M. A., Mora, A., Sevink, J.,
668 Sanmartin, I., Sanchez-Meseguer, A., Anderson, C. L., Figueiredo, J. P., Jaramillo, C., Riff,
669 D., Negri, F. R., Hooghiemstra, H., Lundberg, J., Stadler, T., Sarkinen, T. and Antonelli, A.:
670 Amazonia through time: Andean uplift, climate change, landscape evolution, and biodiversity,
671 *Science*, 330(6006), 927–931, doi:10.1126/science.1194585, 2010.
- 672 Horn, M. H., Correa, S. B., Parolin, P., Pollux, B. J. A., Anderson, J. T., Lucas, C., Widmann,
673 P., Tjiu, A., Galetti, M. and Goulding, M.: Seed dispersal by fishes in tropical and temperate
674 fresh waters: The growing evidence, *Acta Oecologica*, 37, 561–577,
675 doi:10.1016/j.actao.2011.06.004, 2011.
- 676 Houghton, R. A., Skole, D. L., Nobre, C. A., Hackler, J. L., Lawrence, K. T. and
677 Chomentowski, W. H.: Annual fluxes of carbon from deforestation and regrowth in the
678 Brazilian Amazon, *Nature*, 403(6767), 301–304, 2000.
- 679 INPE: Projeto PRODES: Monitoramento da floresta Amazônica Brasileira por satélite.
680 [online] Available from: <http://www.obt.inpe.br/prodes/index.php> (Accessed 28 April 2015),
681 2013.
- 682 Irmiler, U.: Litterfall and nitrogen turnover in an Amazonian blackwater inundation forest,
683 *Plant and Soil*, 67(1–3), 355–358, 1982.
- 684 Johnson, M. S., Lehmann, J., Selva, E. C., Abdo, M., Riha, S. and Couto, E. G.: Organic
685 carbon fluxes within and streamwater exports from headwater catchments in the southern
686 Amazon, *Hydrological Processes*, 20(12), 2599–2614, 2006.

- 687 Junk, W. J.: The central Amazon floodplain - Ecology of a pulsing system, Springer., 1997.
- 688 Junk, W. J. and Wantzen, K. M.: The flood pulse concept: New aspects, approaches and
689 applications - An update, in Proceedings of the Second International Symposium on the
690 Management of large Rivers for Fisheries, edited by R. L. Welcomme and T. Petr, pp. 117–
691 140., 2004.
- 692 Jupp, T. E., Cox, P. M., Rammig, A., Thonicke, K., Lucht, W. and Cramer, W.: Development
693 of probability density functions for future South American rainfall, *New Phytologist*, 187,
694 682–693, doi:10.1111/j.1469-8137.2010.03368.x, 2010.
- 695 Keller, M., Bustamante, M., Gash, J. and Silva Dias, P., Eds.: Amazonia and global change,
696 American Geophysical Union, Washington, DC., 2009.
- 697 Körtzinger, A.: A significant CO₂ sink in the tropical Atlantic Ocean associated with the
698 Amazon River plume, *Geophysical Research Letters*, 30(24), doi:10.1029/2003GL018841,
699 2003.
- 700 Langerwisch, F., Rost, S., Gerten, D., Poulter, B., Rammig, A. and Cramer, W.: Potential
701 effects of climate change on inundation patterns in the Amazon Basin, *Hydrology and Earth
702 System Sciences*, 17(6), 2247–2262, doi:10.5194/hess-17-2247-2013, 2013.
- 703 Langerwisch, F., Walz, A., Rammig, A., Tietjen, B., Thonicke, K. and Cramer, W.: Climate
704 change increases riverine carbon outgassing while export to the ocean remains uncertain,
705 *Earth System Dynamics Discussions*, 6(2), 1445–1497, doi:10.5194/esdd-6-1445-2015, 2015.
- 706 Langerwisch, F., Walz, A., Rammig, A., Tietjen, B., Thonicke, K. and Cramer, W.: Climate
707 change increases riverine carbon outgassing, while export to the ocean remains uncertain,
708 *Earth System Dynamics*, 7(3), 559–582, doi:10.5194/esd-7-559-2016, 2016.
- 709 Lawrence, D. and Vandecar, K.: Effects of tropical deforestation on climate and agriculture,
710 *Nature Climate Change*, 5(1), 27–36, doi:10.1038/nclimate2430, 2014.
- 711 Lewis, S. L., Brando, P. M., Phillips, O. L., van der Heijden, G. M. . and Nepstad, D.: The
712 2010 amazon drought, *Science*, 331(6017), 554, doi:10.1126/science.1200807, 2011.
- 713 Malhi, Y., Wood, D., Baker, T. R., Wright, J., Phillips, O. L., Cochrane, T., Meir, P., Chave,
714 J., Almeida, S., Arroyo, L., Higuchi, N., Killeen, T. J., Laurance, S. G., Laurance, W. F.,
715 Lewis, S. L., Monteagudo, A., Neill, D. A., Vargas, P. N., Pitman, N. C. A., Quesada, C. A.,
716 Salomão, R., Silva, J. N. M., Lezama, A. T., Terborgh, J., Martínez, R. V. and Vinceti, B.:
717 The regional variation of aboveground live biomass in old-growth Amazonian forests, *Global
718 Change Biology*, 12(7), 1107–1138, 2006.
- 719 Malhi, Y., Roberts, J. T., Betts, R. A., Killeen, T. J., Li, W. and Nobre, C. A.: Climate change,
720 deforestation, and the fate of the Amazon, *Science*, 319(5860), 169–172, 2008.
- 721 Malhi, Y., Saatchi, S., Girardin, C. and Aragão, L. E. O. C.: The production, storage, and flow
722 of carbon in Amazonian forests, in Amazonia and Global Change, pp. 355–372, American
723 Geophysical Union, Washington, DC., 2009.
- 724 Mayorga, E., Aufdenkampe, A. K., Masiello, C. A., Krusche, A. V., Hedges, J. I., Quay, P.
725 D., Richey, J. E. and Brown, T. A.: Young organic matter as a source of carbon dioxide

- 726 outgassing from Amazonian rivers, *Nature*, 436(7050), 538–541, doi:10.1038/nature03880,
727 2005.
- 728 McClain, M. E. and Elsenbeer, H.: Terrestrial inputs to Amazon streams and internal
729 biogeochemical processing, in *The Biogeochemistry of the Amazon Basin*, edited by M. E.
730 McClain, R. L. Victoria, and J. E. Richey, pp. 185–208, Oxford University Press, New York.,
731 2001.
- 732 Melack, J. M. and Forsberg, B.: Biogeochemistry of Amazon floodplain lakes and associated
733 wetlands, in *The Biogeochemistry of the Amazon Basin and its Role in a Changing World*,
734 pp. 235–276, Oxford University Press, Eds. McClain, M. E.; Victoria, R. L.; Richey, J. E.,
735 2001.
- 736 Moreira-Turcq, P., Seyler, P., Guyot, J. L. and Etcheber, H.: Exportation of organic carbon
737 from the Amazon River and its main tributaries, *Hydrological Processes*, 17(7), 1329–1344,
738 doi:10.1002/hyp.1287, 2003.
- 739 Nakićenović, N., Davidson, O., Davis, G., Grübler, A., Kram, T., Lebre La Rovere, E., Metz,
740 B., Morita, T., Pepper, W., Pitcher, H., Sankovski, A., Shukla, P., Swart, R. and Dadi, Z.:
741 IPCC Special report on emission scenarios, [online] Available from:
742 <http://www.ipcc.ch/ipccreports/sres/emission/index.php?idp=0>, 2000.
- 743 Nepstad, D., McGrath, D., Stickler, C., Alencar, A., Azevedo, A., Swette, B., Bezerra, T.,
744 DiGiano, M., Shimada, J., Seroa da Motta, R., Armijo, E., Castello, L., Brando, P., Hansen,
745 M. C., McGrath-Horn, M., Carvalho, O. and Hess, L.: Slowing Amazon deforestation through
746 public policy and interventions in beef and soy supply chains, *Science*, 344(6188), 1118–
747 1123, doi:10.1126/science.1248525, 2014.
- 748 Nobre, A. D.: The Future Climate of Amazonia: Scientific Assessment Report, INPA and
749 ARA, São José dos Campos, Brazil. [online] Available from: [http://www.ccst.inpe.br/wp-](http://www.ccst.inpe.br/wp-content/uploads/2014/11/The_Future_Climate_of_Amazonia_Report.pdf)
750 [content/uploads/2014/11/ The_Future_Climate_of_Amazonia_Report.pdf](http://www.ccst.inpe.br/wp-content/uploads/2014/11/The_Future_Climate_of_Amazonia_Report.pdf) (Accessed 31
751 August 2015), 2014.
- 752 Poorter, L., Bongers, F., Aide, T. M., Almeyda Zambrano, A. M., Balvanera, P., Becknell, J.
753 M., Boukili, V., Brancalion, P. H. S., Broadbent, E. N., Chazdon, R. L., Craven, D., de
754 Almeida-Cortez, J. S., Cabral, G. A. L., de Jong, B. H. J., Denslow, J. S., Dent, D. H.,
755 DeWalt, S. J., Dupuy, J. M., Durán, S. M., Espírito-Santo, M. M., Fandino, M. C., César, R.
756 G., Hall, J. S., Hernandez-Stefanoni, J. L., Jakovac, C. C., Junqueira, A. B., Kennard, D.,
757 Letcher, S. G., Licona, J.-C., Lohbeck, M., Marín-Spiotta, E., Martínez-Ramos, M., Massoca,
758 P., Meave, J. A., Mesquita, R., Mora, F., Muñoz, R., Muscarella, R., Nunes, Y. R. F., Ochoa-
759 Gaona, S., de Oliveira, A. A., Orihuela-Belmonte, E., Peña-Claros, M., Pérez-García, E. A.,
760 Piotto, D., Powers, J. S., Rodríguez-Velázquez, J., Romero-Pérez, I. E., Ruíz, J., Saldarriaga,
761 J. G., Sanchez-Azofeifa, A., Schwartz, N. B., Steininger, M. K., Swenson, N. G., Toledo, M.,
762 Uriarte, M., van Breugel, M., van der Wal, H., Veloso, M. D. M., Vester, H. F. M., Vicentini,
763 A., Vieira, I. C. G., Bentos, T. V., Williamson, G. B. and Rozendaal, D. M. A.: Biomass
764 resilience of Neotropical secondary forests, *Nature*, 530(7589), 211–214,
765 doi:10.1038/nature16512, 2016.
- 766 Potter, C., Klooster, S. and Genovese, V.: Carbon emissions from deforestation in the
767 Brazilian Amazon Region, *Biogeosciences*, 6(11), 2369–2381, 2009.

- 768 Randall, D. A., Wood, R. A., Bony, S., Colman, R., Fichefet, T., Fyfe, J., Kattsov, V., Pitman,
769 A., Shukla, J., Srinivasan, J., Stouffer, R. J., Sumi, A. and Taylor, K. E.: Climate models and
770 their evaluation, in *Climate Change 2007: The Physical Science Basis. Contribution of*
771 *Working Group I to the Fourth Assessment Report of the Intergovernmental Panel on Climate*
772 *Change*, edited by S. Solomon, D. Qin, M. Manning, Z. Chen, M. Marquis, K. B. Averyt, M.
773 Tignor, and H. L. Miller, Cambridge University Press., 2007.
- 774 von Randow, C., Manzi, A. O., Kruijt, B., de Oliveira, P. J., Zanchi, F. B., Silva, R. L.,
775 Hodnett, M. G., Gash, J. H. C., Elbers, J. A., Waterloo, M. J., Cardoso, F. L. and Kabat, P.:
776 Comparative measurements and seasonal variations in energy and carbon exchange over
777 forest and pasture in South West Amazonia, *Theoretical and Applied Climatology*, 78(1–3),
778 5–26, doi:10.1007/s00704-004-0041-z, 2004.
- 779 Richey, J. E., Melack, J. M., Aufdenkampe, A. K., Ballester, V. M. and Hess, L. L.:
780 Outgassing from Amazonian rivers and wetlands as a large tropical source of atmospheric
781 CO₂, *Nature*, 416(6881), 617–620, doi:10.1038/416617a, 2002.
- 782 Rost, S., Gerten, D., Bondeau, A., Lucht, W., Rohwer, J. and Schaphoff, S.: Agricultural
783 green and blue water consumption and its influence on the global water system, *Water*
784 *Resources Research*, 44(9), doi:W09405 10.1029/2007wr006331, 2008.
- 785 Sitch, S., Smith, B., Prentice, I. C., Arneth, A., Bondeau, A., Cramer, W., Kaplan, J. O.,
786 Levis, S., Lucht, W., Sykes, M. T., Thonicke, K. and Venevsky, S.: Evaluation of ecosystem
787 dynamics, plant geography and terrestrial carbon cycling in the LPJ dynamic global
788 vegetation model, *Global Change Biology*, 9(2), 161–185, doi:10.1046/j.1365-
789 2486.2003.00569.x, 2003.
- 790 Soares-Filho, B. S., Nepstad, D. C., Curran, L. M., Cerqueira, G. C., Garcia, R. A., Ramos, C.
791 A., Voll, E., McDonald, A., Lefebvre, P. and Schlesinger, P.: Modelling conservation in the
792 Amazon basin, *Nature*, 440(7083), 520–523, 2006.
- 793 Spracklen, D. V., Arnold, S. R. and Taylor, C. M.: Observations of increased tropical rainfall
794 preceded by air passage over forests, *Nature*, 489(7415), 282–285, doi:10.1038/nature11390,
795 2012.
- 796 Subramaniam, A., Yager, P. L., Carpenter, E. J., Mahaffey, C., Bjorkman, K., Cooley, S.,
797 Kustka, A. B., Montoya, J. P., Sanudo-Wilhelmy, S. A., Shipe, R. and Capone, D. G.:
798 Amazon River enhances diazotrophy and carbon sequestration in the tropical North Atlantic
799 Ocean, *Proceedings of the National Academy of Sciences*, 105(30), 10460–10465,
800 doi:10.1073/pnas.0710279105, 2008.
- 801 Thonicke, K., Spessa, A., Prentice, I. C., Harrison, S. P., Dong, L. and Carmona-Moreno, C.:
802 The influence of vegetation, fire spread and fire behaviour on biomass burning and trace gas
803 emissions: results from a process-based model, *Biogeosciences*, 7(6), 1991–2011,
804 doi:10.5194/bg-7-1991-2010, 2010.
- 805 Wagner, W., Scipal, K., Pathe, C., Gerten, D., Lucht, W. and Rudolf, B.: Evaluation of the
806 agreement between the first global remotely sensed soil moisture data with model and
807 precipitation data, *Journal of Geophysical Research*, 108(4611), doi:10.1029/2003JD003663,
808 2003.
- 809 Waterloo, M. J., Oliveira, S. M., Drucker, D. P., Nobre, A. D., Cuartas, L. A., Hodnett, M. G.,
810 Langedijk, I., Jans, W. W. P., Tomasella, J., de Araújo, A. C., Pimentel, T. P. and Estrada, J.

- 811 C. M.: Export of organic carbon in run-off from an Amazonian rainforest blackwater
812 catchment, *Hydrological Processes*, 20(12), 2581–2597, 2006.
- 813 Worbes, M.: The forest ecosystem of the floodplains, in *The Central Amazon Floodplain*,
814 edited by W. J. Junk, pp. 223–265, Springer, Berlin, Germany., 1997.
- 815 Yang, D., Kanae, S., Oki, T., Koike, T. and Musiaka, K.: Global potential soil erosion with
816 reference to land use and climate changes, *Hydrological Processes*, 17(14), 2913–2928,
817 doi:10.1002/hyp.1441, 2003.
- 818
- 819

820

821 **7 Tables**

822 **Table 1: Location and characteristics of the three sub-regions.**

| | <i>North-West corner</i> | <i>South-East corner</i> | <i>area [10³km²]</i> | <i>changes in inundation length*</i> | <i>changes inundated area*</i> | <i>land use intensity</i> |
|----|--------------------------|--------------------------|--|--------------------------------------|--------------------------------|---------------------------|
| R1 | 0.5°S / 78.5°W | 7.0°S / 72°W | 523.03 | 1 month longer | larger | low |
| R2 | 1.0°S / 70.0°W | 5.0°S / 52°W | 891.32 | ±½ month shift | heterogeneous | medium |
| R3 | 4.5°S / 58.0°W | 11.0°S / 52°W | 523.03 | ½ month shorter | smaller | high |

823 Regions are depicted in **Figure 2.** * Changes in inundation compared to the average of 1961-
824 1990, as estimated and discussed in Langerwisch et al. (2013)

825

826

827 **Table 2: Basin-wide (B) and region wise (R1-R3) amount of carbon in POC and DOC,**
 828 **outgassed carbon and IC [10^{12} g month⁻¹] averaged over 30 years and five climate**
 829 **models.**

| | NatVeg _{ref} | NatVeg _{fut} | GOV _{futA/B} | BAU _{futA/B} | GOV _{futA2} | BAU _{futA2} | GOV _{futB1} | BAU _{futB1} |
|-------------------------|-----------------------|-----------------------|-----------------------|-----------------------|----------------------|----------------------|----------------------|----------------------|
| POC | | | | | | | | |
| B | 1.64±0.06 | 1.76±0.51 | 1.52±0.43 | 1.28±0.35 | 1.63±0.41 | 1.39±0.34 | 1.55±0.31 | 1.30±0.24 |
| R1 | 0.16±0.01 | 0.22±0.05 | 0.20±0.05 | 0.20±0.05 | 0.21±0.05 | 0.21±0.05 | 0.18±0.02 | 0.18±0.02 |
| R2 | 0.42±0.01 | 0.43±0.15 | 0.37±0.12 | 0.30±0.09 | 0.40±0.13 | 0.33±0.10 | 0.38±0.09 | 0.31±0.07 |
| R3 | 0.15±0.01 | 0.14±0.05 | 0.11±0.04 | 0.07±0.03 | 0.12±0.04 | 0.08±0.02 | 0.12±0.03 | 0.08±0.02 |
| DOC | | | | | | | | |
| B | 3.41±0.13 | 3.58±1.05 | 3.07±0.87 | 2.59±0.71 | 3.29±0.84 | 2.77±0.69 | 3.15±0.63 | 2.64±0.48 |
| R1 | 0.34±0.02 | 0.46±0.11 | 0.43±0.10 | 0.42±0.10 | 0.45±0.10 | 0.44±0.10 | 0.39±0.05 | 0.38±0.05 |
| R2 | 0.93±0.03 | 0.91±0.32 | 0.77±0.26 | 0.64±0.20 | 0.84±0.27 | 0.69±0.21 | 0.81±0.20 | 0.66±0.15 |
| R3 | 0.34±0.02 | 0.30±0.11 | 0.24±0.09 | 0.16±0.06 | 0.26±0.08 | 0.17±0.05 | 0.27±0.07 | 0.17±0.04 |
| outgassed carbon | | | | | | | | |
| B | 11.82±0.41 | 16.63±4.14 | 14.30±3.44 | 12.05±2.76 | 15.75±3.43 | 13.24±2.80 | 13.37±2.20 | 11.15±1.68 |
| R1 | 1.15±0.06 | 2.05±0.38 | 1.93±0.35 | 1.91±0.35 | 2.10±0.35 | 2.08±0.35 | 1.61±0.13 | 1.60±0.14 |
| R2 | 2.52±0.08 | 3.36±0.99 | 2.81±0.78 | 2.37±0.6 | 3.09±0.85 | 2.59±0.66 | 2.66±0.56 | 2.22±0.43 |
| R3 | 0.99±0.04 | 1.12±0.42 | 0.91±0.34 | 0.55±0.20 | 1.03±0.32 | 0.62±0.18 | 0.94±0.26 | 0.56±0.14 |
| IC | | | | | | | | |
| B | 0.227±0.003 | 0.457±0.119 | 0.457±0.120 | 0.456±0.121 | 0.523±0.137 | 0.522±0.138 | 0.365±0.063 | 0.364±0.064 |
| R1 | 0.005±0.001 | 0.016±0.003 | 0.013±0.003 | 0.013±0.003 | 0.015±0.004 | 0.015±0.004 | 0.009±0.001 | 0.009±0.001 |
| R2 | 0.153±0.002 | 0.308±0.081 | 0.308±0.082 | 0.307±0.083 | 0.351±0.094 | 0.350±0.096 | 0.245±0.044 | 0.244±0.044 |
| R3 | 0.006±0.000 | 0.011±0.003 | 0.011±0.003 | 0.011±0.003 | 0.013±0.003 | 0.013±0.003 | 0.009±0.001 | 0.009±0.001 |

830 'ref' refers to mean amounts during reference period 1971-2000. 'fut' refers to mean amounts
 831 during future period 2070-2099. Values given are the mean ± standard deviation of the five
 832 climate models.

833

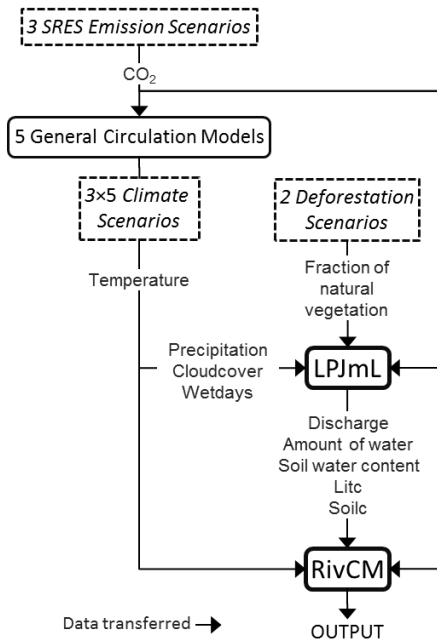
834

835 **Table 3: Proportion [%] of area dominated by climate or land use change impacts.**

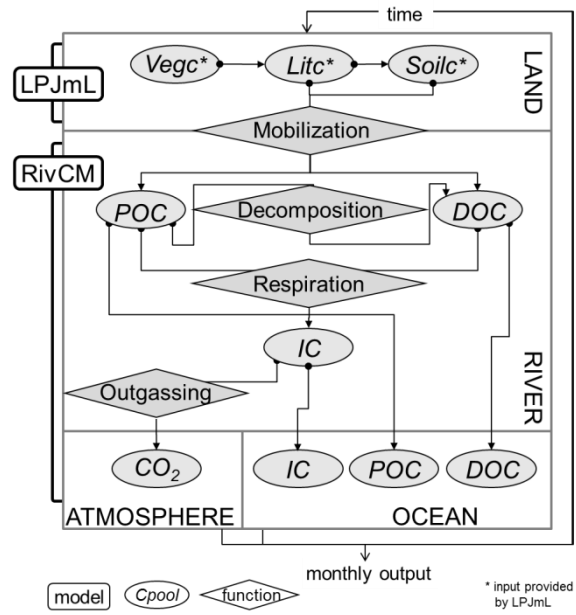
| | <i>significantly changed fraction</i> | | | <i>climate change dominated¹</i> | | | <i>land use change dominated¹</i> | | | <i>balanced¹</i> | | |
|-------------------------|---------------------------------------|-----------|-----------|---|-----------|-----------|--|-----------|-----------|-----------------------------|-----------|-----------|
| | <i>A1B</i> | <i>A2</i> | <i>B1</i> | <i>A1B</i> | <i>A2</i> | <i>B1</i> | <i>A1B</i> | <i>A2</i> | <i>B1</i> | <i>A1B</i> | <i>A2</i> | <i>B1</i> |
| POC | | | | | | | | | | | | |
| GOV | 50.85 | 50.91 | 50.86 | 58.8 | 58.7 | 54.9 | 40.9 | 40.7 | 44.6 | 0.3 | 0.6 | 0.5 |
| BAU | 50.80 | 50.85 | 50.85 | 42.3 | 43.7 | 40.1 | 57.5 | 56.2 | 59.8 | 0.2 | 0.1 | 0.1 |
| IC | | | | | | | | | | | | |
| GOV | 50.80 | 50.80 | 50.80 | 100.0 | 100.0 | 100.0 | 0.0 | 0.0 | 0.0 | 0.0 | 0.0 | 0.0 |
| BAU | 50.80 | 50.80 | 50.80 | 100.0 | 100.0 | 100.0 | 0.0 | 0.0 | 0.0 | 0.0 | 0.0 | 0.0 |
| outgassed carbon | | | | | | | | | | | | |
| GOV | 97.6 | 97.60 | 97.61 | 70.5 | 77.7 | 68.4 | 29.3 | 22.3 | 31.1 | 0.2 | 0.0 | 0.4 |
| BAU | 97.55 | 97.65 | 97.60 | 52.4 | 56.9 | 50.2 | 47.6 | 43.0 | 49.7 | 0.1 | 0.1 | 0.1 |

836 If both impacts compensate each other the cell is balanced. ¹The proportions refer to the
837 significantly changed overall fraction (first columns).

A

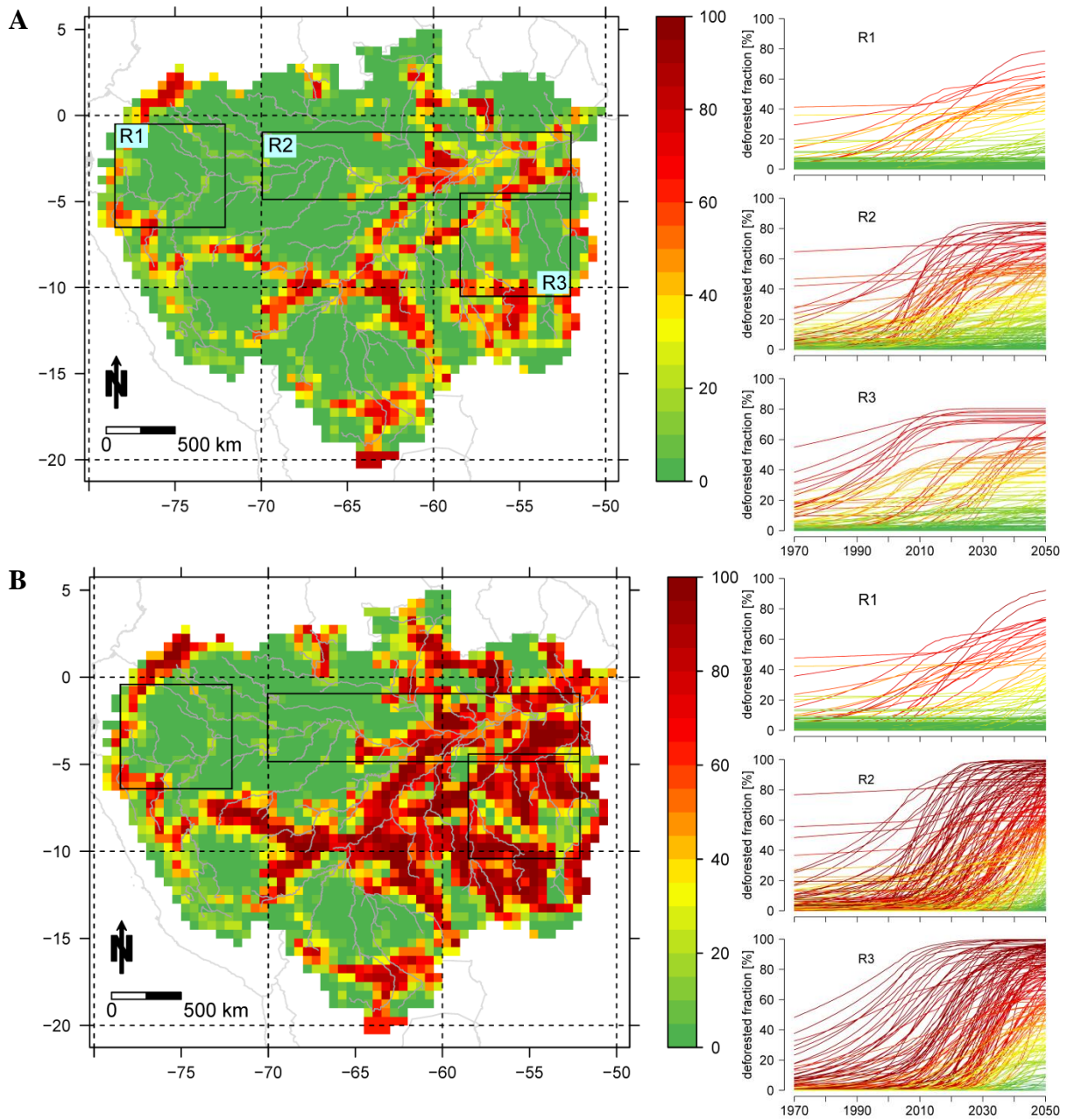


B

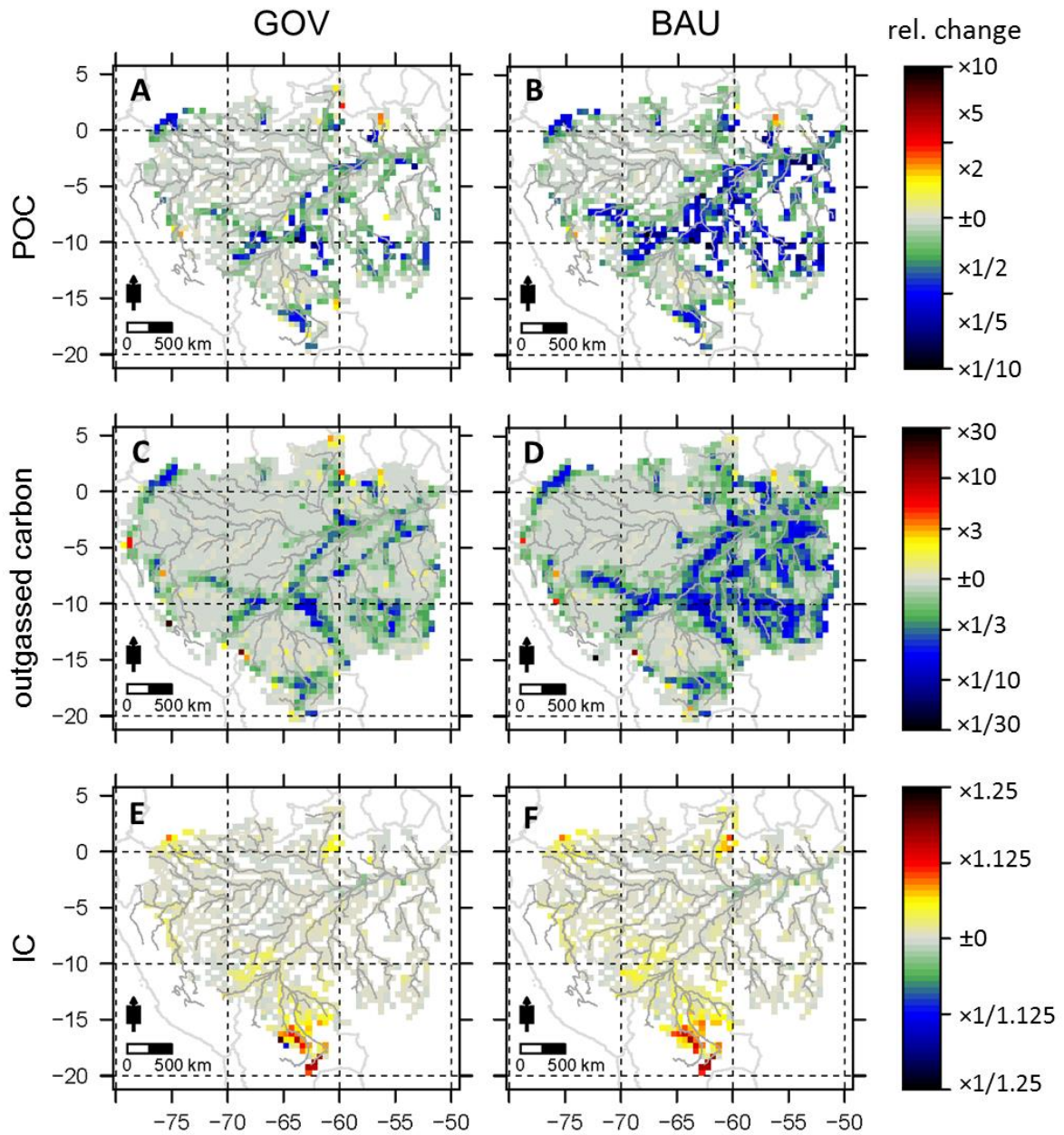


839

840 **Figure 1: Overview of the general transfer of data between scenarios and models (A)**
 841 **and the detailed calculation of carbon fluxes within and between LPJmL and RivCM.**
 842

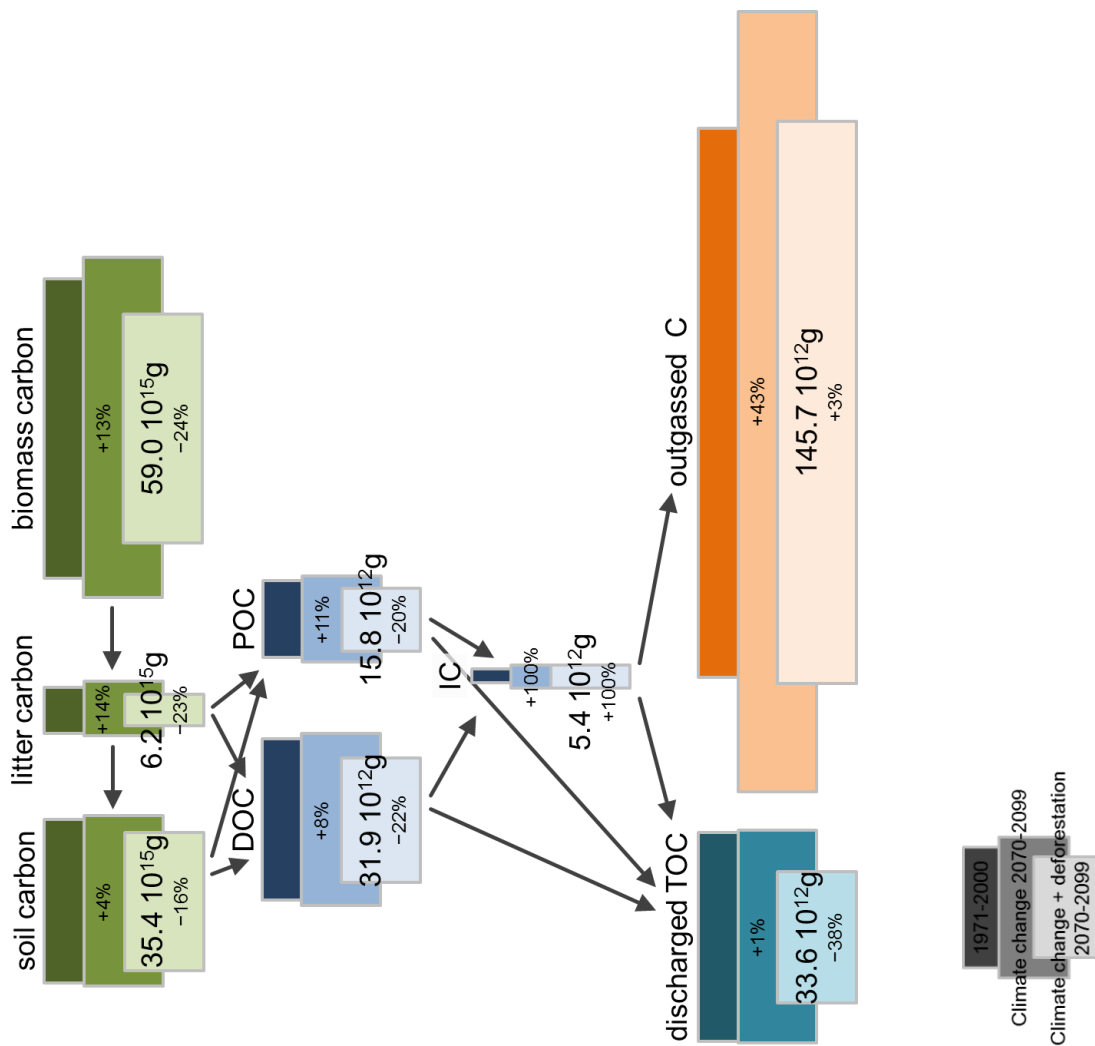


844 **Figure 2: Fraction of deforested area per cell [%] in 2050.** Data are based on Soares-Filho
 845 et al. (2006). Panel A refers to the BAU deforestation scenario, whereas panel B refers to the
 846 GOV scenario. The three sub-regions discussed in the main text are highlighted in the map.
 847 The timelines (right panels) show the development until 2050 for each sub-region
 848 (deforestation kept constant after 2050).



849

850 **Figure 3: Change in carbon caused by deforestation.** Climate model mean (E_{Defor}) of the
 851 change of particulate organic carbon POC (A, B), outgassed carbon (C, D) and inorganic
 852 carbon IC (E, F). Results of the SRES emission scenario A1B are averaged over five climate
 853 models. Areas in yellow and red indicate a gain and areas in green and blue indicate a loss in
 854 carbon caused by deforestation (GOV and BAU). White areas within the Amazon basin
 855 represent cells where changes are not significant (p -value > 0.05).

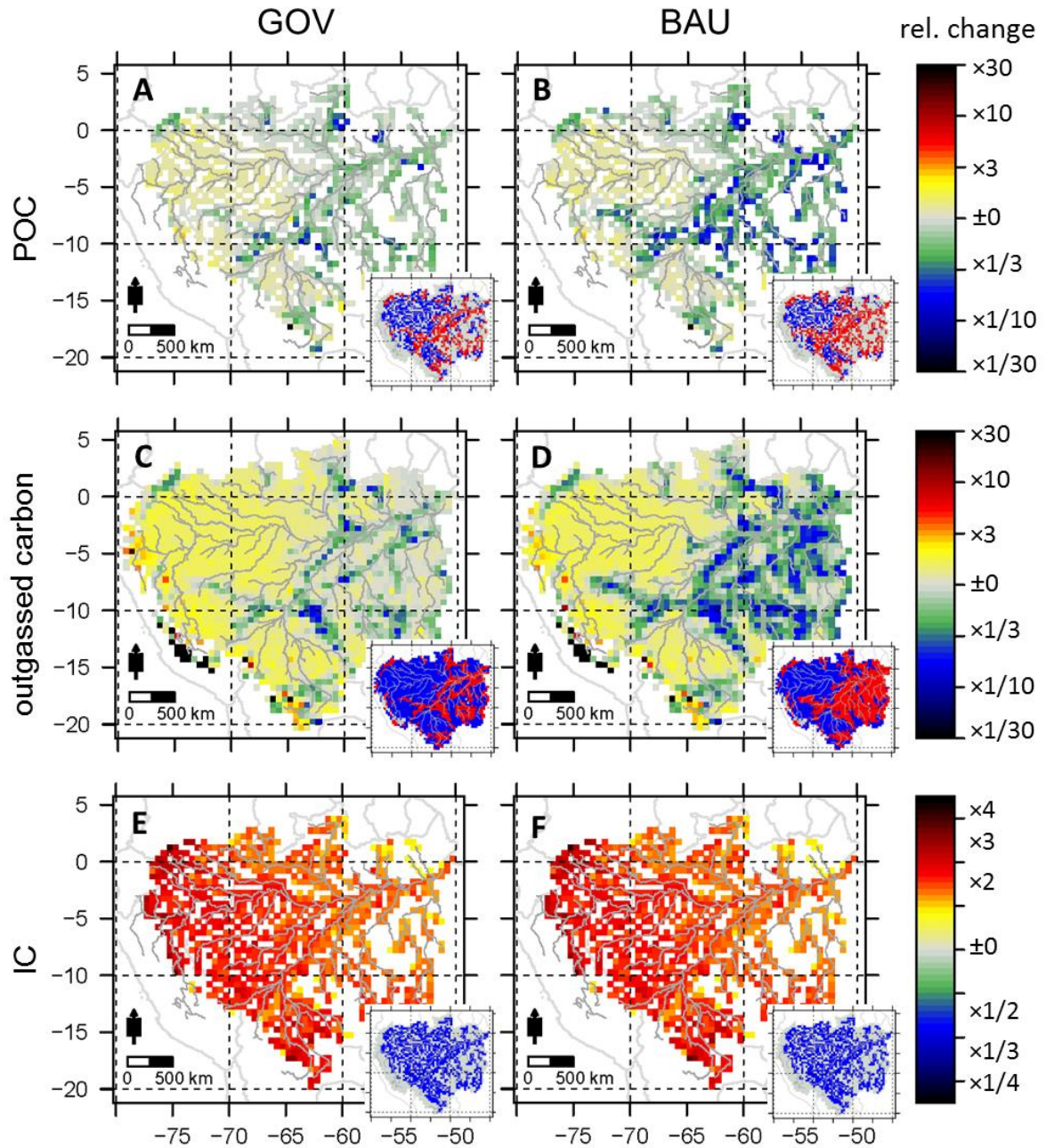


857

858 **Figure 4: Averaged annual amounts and change in the basin carbon budget due to**
 859 **climate change and deforestation.** Dark boxes indicate the amount of carbon during the
 860 reference period (1971-2000), intermediate boxes during the future period (2070-2099) under
 861 climate change only (Langerwisch et al., 2015), light boxes during the future period under the
 862 forcing of climate change and deforestation (BAU) together (average over all SRES scenarios
 863 and GCMs). Amount is given for future period with relative change compared to reference.
 864 Arrows indicate the direction of carbon transfer.

865

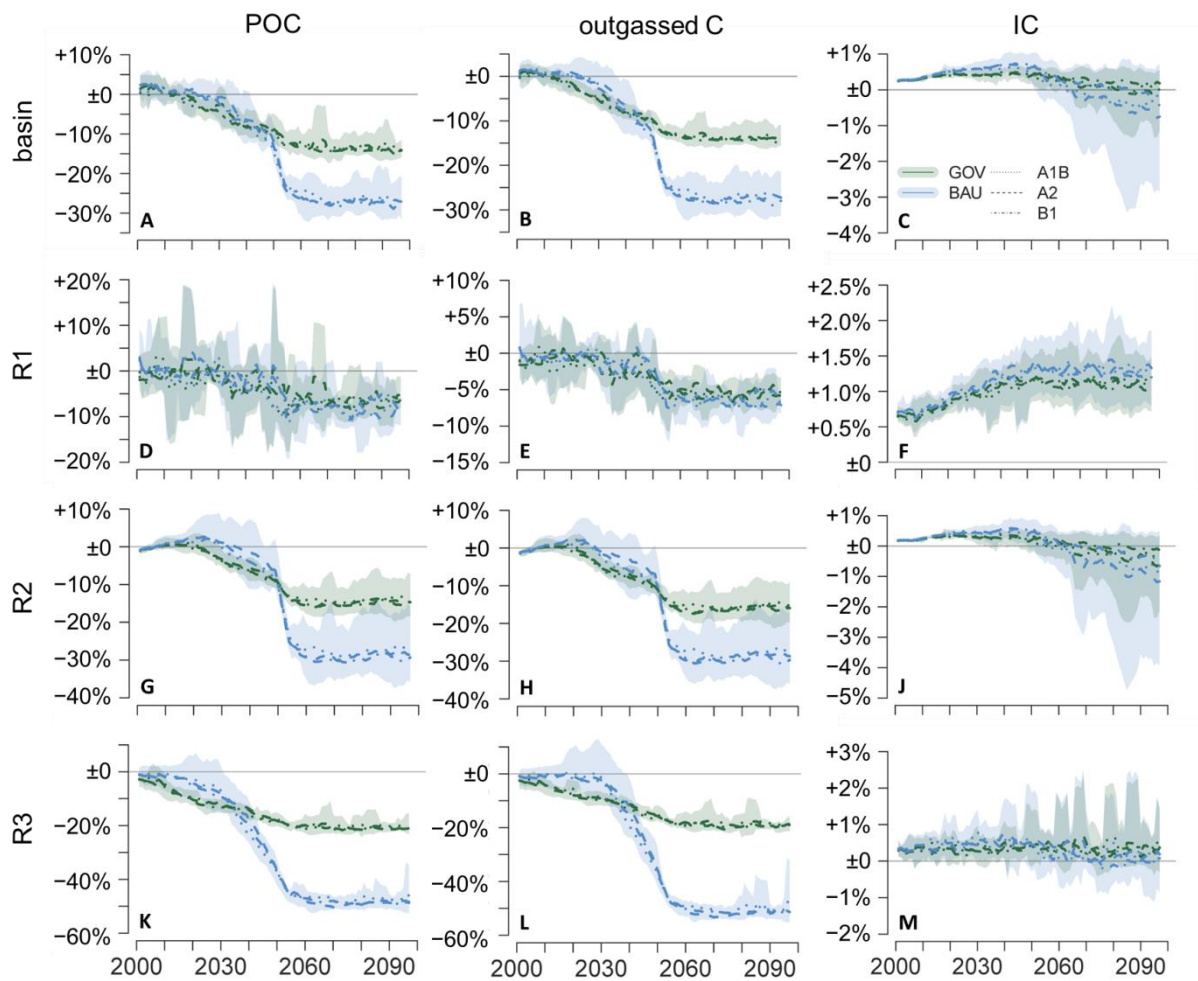
866



867

868 **Figure 5: Change in carbon caused by deforestation and climate change.** Climate model
 869 mean ($E_{CCDefor}$) of the change of particulate organic carbon POC (A, B), outgassed carbon (C,
 870 D) and inorganic carbon IC (E, F). The inset maps show blue areas where changes are
 871 predominantly caused by climate change (D_{CC}) and red areas where changes are
 872 predominantly caused by deforestation (D_{Defor}). For further details see Figure 3. White areas
 873 within the Amazon basin represent cells where changes are not significant (p -value >0.05).

874



876

877 **Figure 6: Temporal change in riverine organic carbon due to land use change only.**
 878 Change of annual sum of carbon in the deforestation scenario (GOV or BAU) compared to the
 879 NatVeg scenario for the whole basin (A-C) and the three sub-regions (R1-R3; D-M) as 5-
 880 year-mean for GOV (green) and BAU (blue), representing E_{Defor} . The shaded areas indicate
 881 the full range of values of all five climate models. Bold lines represent the 5-year-mean of the
 882 five climate models.

883